Karaelmas Science and Engineering Journal
Journal home page: http://fbd.beun.edu.tr
DOI: 10.7212%2Fzkufbd.v8i1.1122

Research Article
Received / Geliş tarihi : 25.09.2017
Accepted / Kabul tarihi : 09.11.2017

ZnO Films Obtained by Electrodeposition Under Alternating Magnetic Field

Alternatif Manyetik Alan Altında Elektrodepozisyon ile Üretilen ZnO Filmleri

Barış Altıokka[1*], Ayça Kıyak Yıldırım[2]

Bilecik Şeyh Edebali University, Vocational School, Department of Electricity and Energy, Bilecik, Turkey
Bilecik Şeyh Edebali University, Vocational School, Department of Motor Vehicles and Transportatıon Technologies, Bilecik, Turkey

Abstract

Thin films of polycrystalline ZnO were produced by electrodeposition under alternating magnetic field. The structures of the films deposited under a magnetic field were defined by X-ray diffractometer (XRD) and it revealed that the films formed in a hexagonal structure. The energy gaps of the films produced without magnetic field were estimated between 3.54 eV and 3.63 eV while the others varied from the 3.60 eV to the 3.79 eV.

Keywords: Electrodeposition, Magnetic field, Thin film, ZnO

Öz

Polikristal ZnO ince filmleri alternatif manyetik alan altında elektrodepozisyon ile üretildiler. Manyetik alan altında üretilen filmlerin yapıları X-ray cihazı (XRD) ile araştırıldı ve bu sonuçlar filmlerin hegzagonal oluştuklarını gösterdi. Manyetik alansız üretilen filmlerin enerji bant aralıkları 3.54 eV ve 3.63 eV aralığında tahmin edilirken diğerlerinin 3.60 eV'den 3.79 eV'ye değiştikleri anlaşıldı.

Anahtar Kelimeler: Elektrodepozisyon, Manyetik alan, İnce film, ZnO

1. Introduction

Zinc Oxide (ZnO) has been attracting an increasing amount of attentions in many fields because of its wide direct band gap of 3.37 eV at room temperature and large excitation binding energy of 60 meV (Henni et al. 2016). ZnO forms in three different structures such as hexagonal wurtzite, cubic zinc blend and seldom in cubic rock salt. Wurtzite form is the most general structure and the zinc blend form can be obtained on substrate of which structure is cubic lattice. The rock salt form can be seen only relatively high pressure of 10 GPa (Ezenwa 2012).

ZnO has attracted great interest over the last few years due to its unique physical properties and wide range of applications such as electro-optical, ferroelectric, pyroelectric and piezoelectric (Zhang et al. 2014). These applications include optoelectronic devices (Wei et al. 2012), antireflection coating transparent electrodes in solar cells, thin films transistors, sensors, surface acoustic wave device, light emitting diodes, microfluidic actuators (Wen-Bo et al. 2015). ZnO has high aspect ratio of atoms because of this features ZnO nanostructures especially are used dye sensitized solarcells, field effect transistors, targeted drug delivery, anticancer agents and antibacterial activity (Jan et al. 2013).

Various kinds of nanostructures of ZnO such as nanorods, nanowalls, nanowires, nanobelt, nanotower and nanocomp (Sun et al. 2012) can be synthesized by different methods, such as sypray pyrolysis, atomic layer epitaxy, sol-gel, pulsed laser deposition, RF magnetron sputtering, electrodeposition (Zhang et al. 2014), metal organic chemical vapor deposition, chemical bath deposition (Altıokka and Kıyak Yıldırım 2016), hydrothermal synthesis, radio frequency plasma, thermal evaporation, oxidation and anodizing (AlArfaj and Subahi 2015). Among these methods, electrodeposition is widely used in the laboratory and industrial production because of many advantages such as simple process, cost-efficiency, large-area deposition, and the easy control of surface morphology and thickness of film (Henni et al. 2016). In the literature, films are also obtained under electromagnetic radiation, electrical field or DC magnetic

*Corresponding author: baltiokka@gmail.com

Barış Altıokka orcid.org/0000-0001-8891-973X
Ayça Kıyak Yıldırım orcid.org/0000-0002-8339-947X

field for control of size, morphology and nanostructure. Magnetic field plays a role of external factor that influences the growth of thin films such as deposition from different types of electrodeposition (AlArfaj and Subahi 2015).

ZnO formation mechanisms were given following Equations (Park et al. 2015).

$$ZnCl_2 \leftrightarrow Zn^{2+} + 2Cl^- \quad (1)$$

$$O_2 + 2H_2O + 4e^- \rightarrow 4OH^- \quad (2)$$

$$Zn^{2+} + 2OH^- \rightarrow Zn(OH)_2 \quad (3)$$

$$Zn(OH)_2 \rightarrow ZnO + H_2O \quad (4)$$

In a previously study, ZnO films have been produced under a alternating magnetic but $Zn(NO_3)_2$ was used as an electrolyte and effects of magnetic field were searched only -0.9 V cathodic potential.

In this study, $ZnCl_2$ was used as an electrolyte and for the first time effects of magnetic field were searched at different cathodic potentials ranging from -0.8 V to the -1.16 V. It was found that alternating magnetic field increased energy band gap of the films from 3.54 eV up to 3.79 eV depending on decreasing of cathodic potential. The effects of magnetic fields on the some of the physical properties were investigated at different cathodic potentials.

2. Materials and Method

ZnO films were electrodeposited onto glass substrates whose surface coated with indium tin oxide (ITO). The electrodeposition procedure taken place with three-electrode which were saturated calomel electrode, a platinum wire and working electrode in using an aqueous solution of containing 0.05 M$ZnCl_2$ and 0.1 M KCl as supporting electrolyte. In the all experiments, substrates (25 Ω/sq) were sunk in the solutions as to be perpendicular to the magnetic field. The substrates were cleaned in acetone, then ethanol (95%) for 5 minutes followed by rinsing with deionized water, and then, they were dried in ambient air before the depositions. The pHs of the final aqueous solutions were measured as to be 5.35. Before the depositions, aqueous solutions were saturated by oxygen for 30 minutes then stirred at 600 rpm and the temperature was kept at a constant value of 70°C during the depositions. The experiments were separated in two main groups. One of the two group samples were deposited without the magnetic field and named as S1, S2, S3, S4 and S5 according to cathodic potentials of -0.8, -0.9, -0.99, -1,05 and -1.16 V respectively. In the other main group, samples were produced under alternating magnetic field which was described in detail in a previous study as to be modified method (Altıokka and Kıyak Yıldırım 2016). In the modified method, samples were deposited under alternating magnetic field a constant value of 6.5 mT and experiments were named as M1, M2, M3, M4 and M5 according to cathodic potentials of -0.8, -0.9, -0.99, -1,05 and -1.16 V respectively. The conditions of the experiment are summarized in Table 1.

The amplitudes of the magnetic fields and the structural properties were analyzed by using a Unilab teslameter and a PANalytical Empyrean XRD respectively. The optical properties of the ZnO films were analyzed by using absorbance measurements for both groups with JASCO V–530 UV-vis. The surface morphology of the ZnO films were investigated by a Zeiss SUPRA 40VP SEM.

Table 1. The Summarized Depositions Conditions

Experiment	Voltage (V)	Magnetic field(mT)	Deposition Temperature (°C)	Deposition Time (sec)	Stirring rpm	pH
S1	-0.80	0	70±2	1800	600	6.28
S2	-0.90	0	70±2	1800	600	6.28
S3	-0.99	0	70±2	1800	600	6.28
S4	-1.05	0	70±2	1800	600	6.28
S5	-1.16	0	70±2	1800	600	6.28
M1	-0.80	6.5mT	70±2	1800	600	6.28
M2	-0.90	6.5mT	70±2	1800	600	6.28
M3	-0.99	6.5mT	70±2	1800	600	6.28
M4	-1.05	6.5mT	70±2	1800	600	6.28
M5	-1.16	6.5mT	70±2	1800	600	6.28

3. Results and Discussion

3.1 X ray diffraction analysis

The current density curves during the electrodeposition process for S series and M series are shown in Figure 1 and Figure 2 respectively. In the both groups, the films thickness can be calculated using Faraday's law which is given the following formula:

$$t = \frac{1}{nFA}\left(\frac{QM}{\rho}\right) \quad (5)$$

where Q is the charge, n is the number of electrons transferred, A is the surface area, F is Faraday's number, ρ is the density (5.6 g/cm^3) and M is the 81.4 g/mol for ZnO (Valdés et al. 2010). These thicknesses are the approximate values because of the fact that the current efficiency during the electrodeposition process is assumed to be 100%. Due to the approach the film thicknesses also were calculated gravimetric method. The calculated film thicknesses from the both groups are given in Table 2. When Table 2 is analyzed, the film thicknesses are increased depend on the increasing cathodic potential and it was seen that the thicknesses of the film obtained in both groups are the approximately same.

Figure 3shows the X-ray diffraction patterns of ZnO films deposited without the magnetic field and shows seven peaks and these peaks are due to the diffraction of (010), (002), (011), (012), (110), (013) and (112) planes. All the diffraction indexed to the hexagonal structure of ZnO.

Figure 4 shows the X-ray diffraction patterns of ZnO films deposited under the magnetic field and shows seven peaks and these peaks are due to the diffraction of (010), (002), (011), (012), (013), (110) and (112) planes. All the diffraction peaks link to the hexagonal structure of ZnO. The texture coefficients of the films deposited under alternating magnetic field are given in Table 4. The preferred orientation of the film obtained in M5 is the (001) while

Table 2. The film thicknesses, band gaps and crystallite sizes of the ZnO films

Experiment	Thickness Faraday law (nm)	Thicknesses Gravimetric (nm)	Eg (eV)	Cristallite Size
S1	578	424	3.54	48
S2	978	790	3.62	40
S3	1190	901	3,63	40
S4	1446	1167	3.56	47
S5	2592	1332	3.50	46
M1	543	409	3.79	35
M2	833	787	3.76	36
M3	1419	964	3.73	37
M4	1517	1190	3.67	39
M5	4269	1355	3.60	40

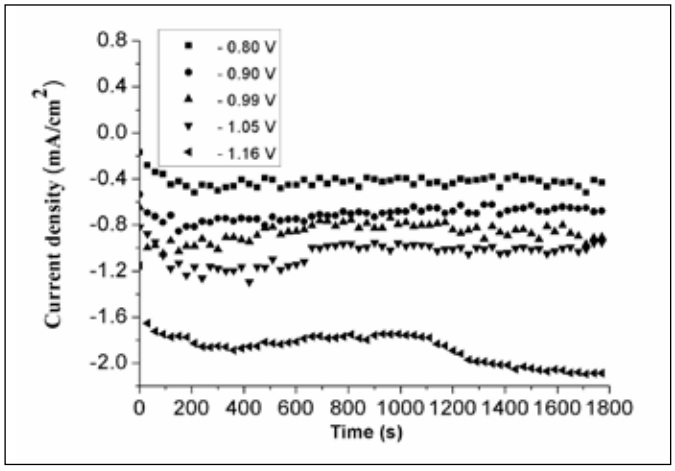

Figure 1. Current densty vs. time of S group.

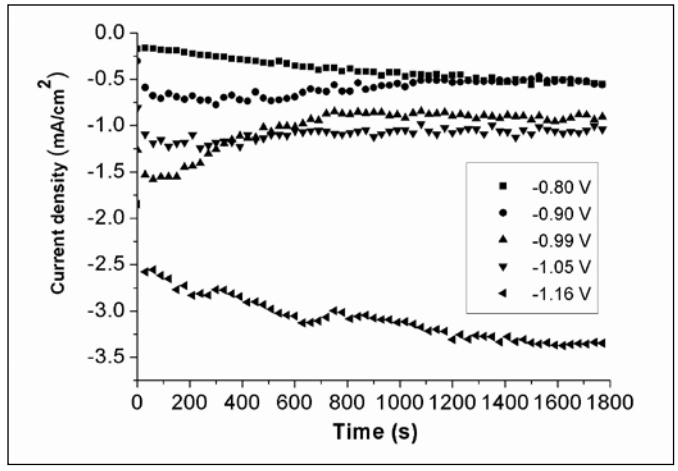

Figure 2. Current densty vs. time of M group.

that of the others are (002) except for film obtained in M1.

The peak intensities of the films produced in S2, S3 and S4 are higher than that of the other films obtained in this group. XRD pattern results shows S1,S2,S3 and S4 have only one intense diffraction peak that located at average 34° indicating that (002) is the preferential crystal orientation.

The Scherrer method is used to calculate crystallite sizes and it is given by Eq. 6.

$$D = \frac{K \times \lambda}{\beta \times \cos\theta} \quad (6)$$

Where D is the crystallite size, λ is the wavelength of X-ray radiation, β is the (FWHM) full with half maximum of peak height, θ is the Bragg's angle and *K* is the Scherrer constant (Mahdi et al. 2015). The crystallite sizes were calculated Sherrer equation and seen in Table 2. The crystallites sizes of the films obtained in S series are varying between 40 and 48 nm while that of the films obtained in M series vary from 35 nm to 40 nm depending on the increasing cathodic voltage. It was concluded that magnetic field effect the formation of crystal and correspondingly crystallite sizes.

3.2 Optical Properties of the Films

The optical properties of the films were analyzed by using absorbance measurements at wavelengths ranging from 300 nm to 600 nm. The absorbance measurements versus wavelength of the films obtained in S series and M series are given in Figure 5a and 5b respectively. The films which were obtained in without magnetic field show high absorbance at wavelength of average 360 nm. On the other hand the films which were obtained under the magnetic field show high absorbance at wavelength of average 350 nm.

Figure 6a and Figure 6b shows the transmittances of the ZnO films produced without magnetic field and under the magnetic field respectively. It is understood from Figure 6 that the ZnO films obtained at -0.90 and -0.99 V show relatively high transmittance while the others show average 15% transmittance. These results may be resulted from both

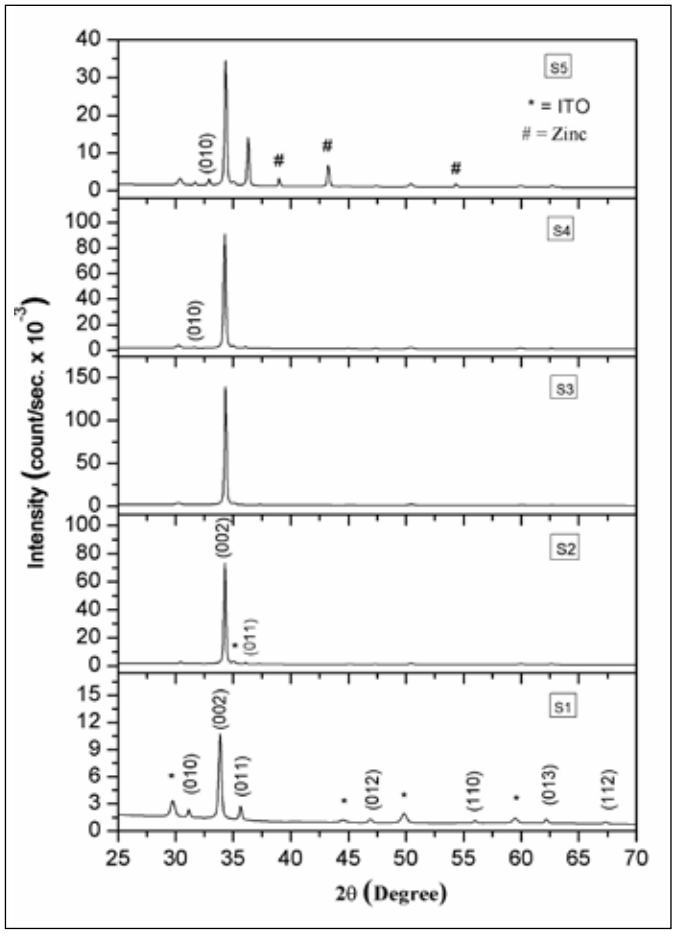

Figure 3. X-ray diffraction patterns of the ZnO films produced in S group.

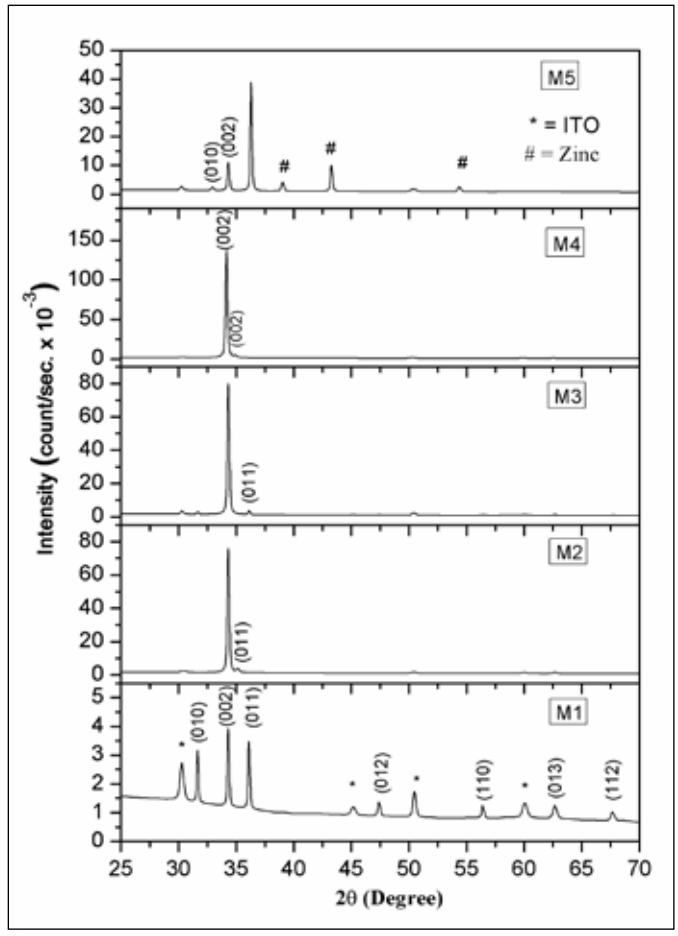

Figure 4. X-ray diffraction patterns of the ZnO films produced in M group.

good crystallization and relatively low film thicknesses of ZnO films. The thicknesses of the films obtained at -0.80 V are also relatively low but crystalization of these films are relatively poor therefore these films show low transmittance

The optical energy gaps of ZnO the films were calculated Tauc relation which is given in Eq. 7 for direct allowed transition.

$$(\alpha hv)^2 = A(hv - Eg) \quad (7)$$

Where α is the absorption coefficient, A is a constant, hν is the photon energy, and Eg is the band-gap (Yilmaz et al. 2012). The Tauc plots of the films obtained in without magnetic field and under the magnetic field are given in Figure 7a and 7b respectively.

The band gaps were calculated using a graphical plot of $(\alpha h\nu)^2$ versus hν given in Fig 7a and 7b.The extrapolation of the curves to the energy axis gave band gaps of between 3.50 eV and 3.63 eV for ZnO nanocrystals obtained in without magnetic field which are listed in Table 2. These values didn't show any relation between the band gaps and chatodic voltages. The band gaps of the films produced under magnetic field increased proportionally from the 3.60 eV to the 3.79 eV according to the decreasing cathodic voltage. These results showed that the magnetic field increased band gaps of the films due to decreasing crystallite size. As the cathodic potential increased the effects of magnetic field decreased and the crystallite size increased accordingly.

3.3 Surface Morphologies of the Films

Surface morphologies of the films were analyzed by using a SEM with coated platinum. The surfaces were magnified both 10000X and 50000X and these two images were given in single figure. The surface images of the films obtained in S series were given in Figure 8 for different cathodic voltages.

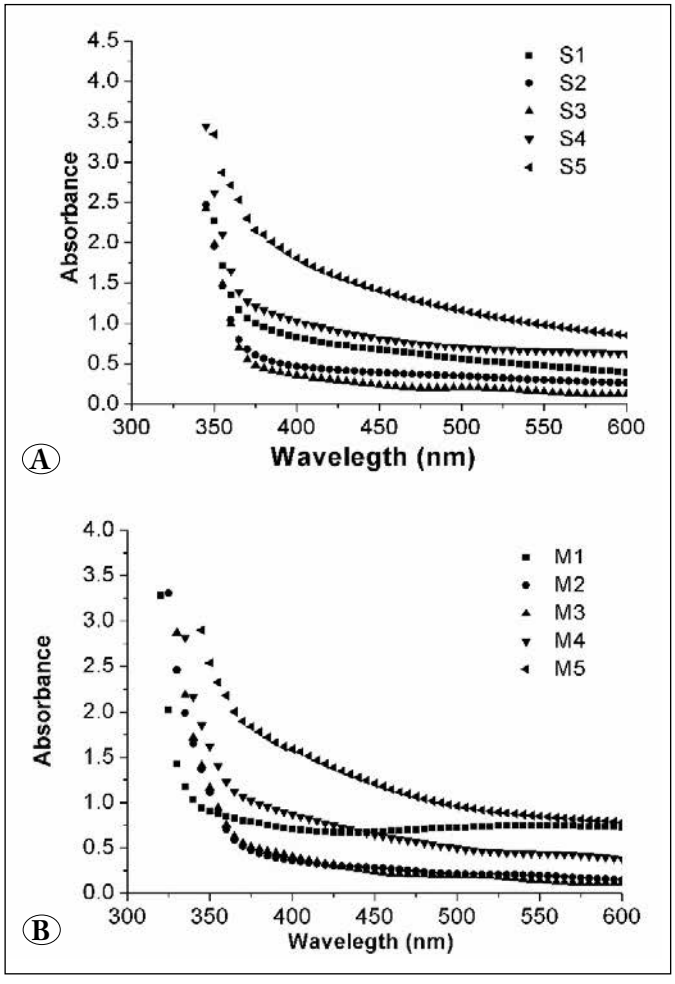

Figure 5. Optical absorption spectra of the ZnO films vs. wavelength range 300 to 600 nm **A)** of the S group **B)** of the M group.

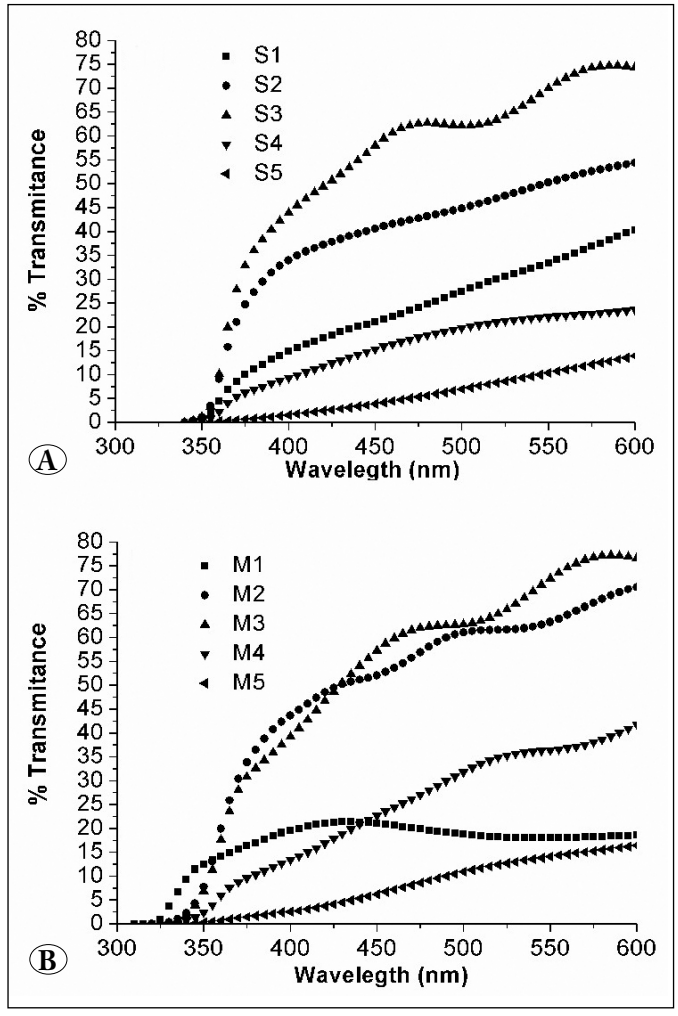

Figure 6. Transmittance spectras vs. vawelength of the ZnO films produced in **A)** S and **B)** M group.

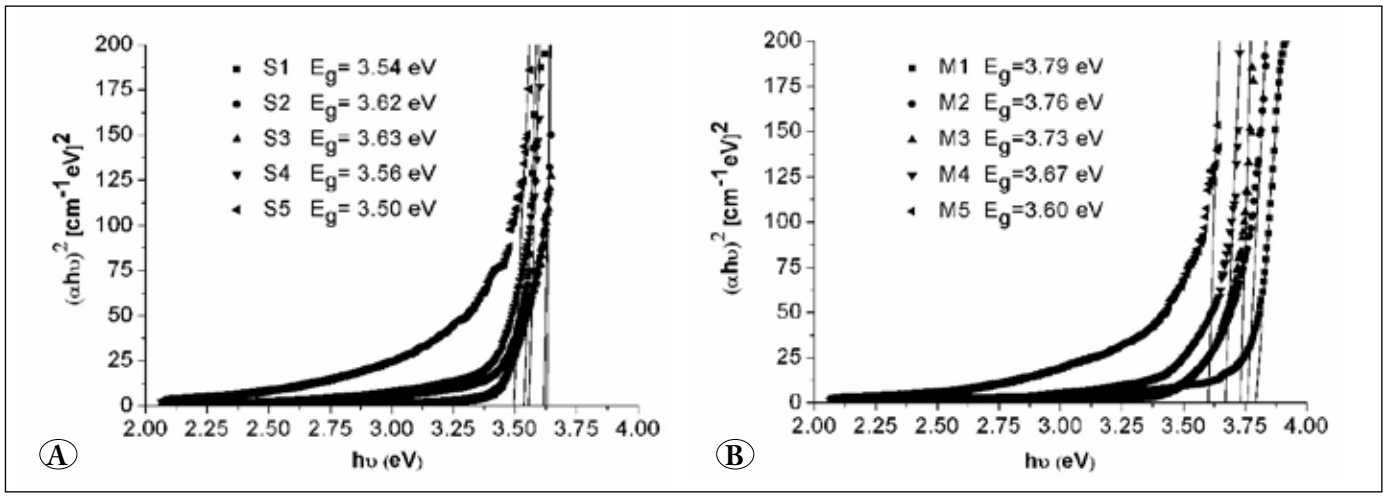

Figure 7. Plots of $(\alpha h\nu)^2$ vs. $h\nu$ for the ZnO films produced in **A)** S and **B)** M group.

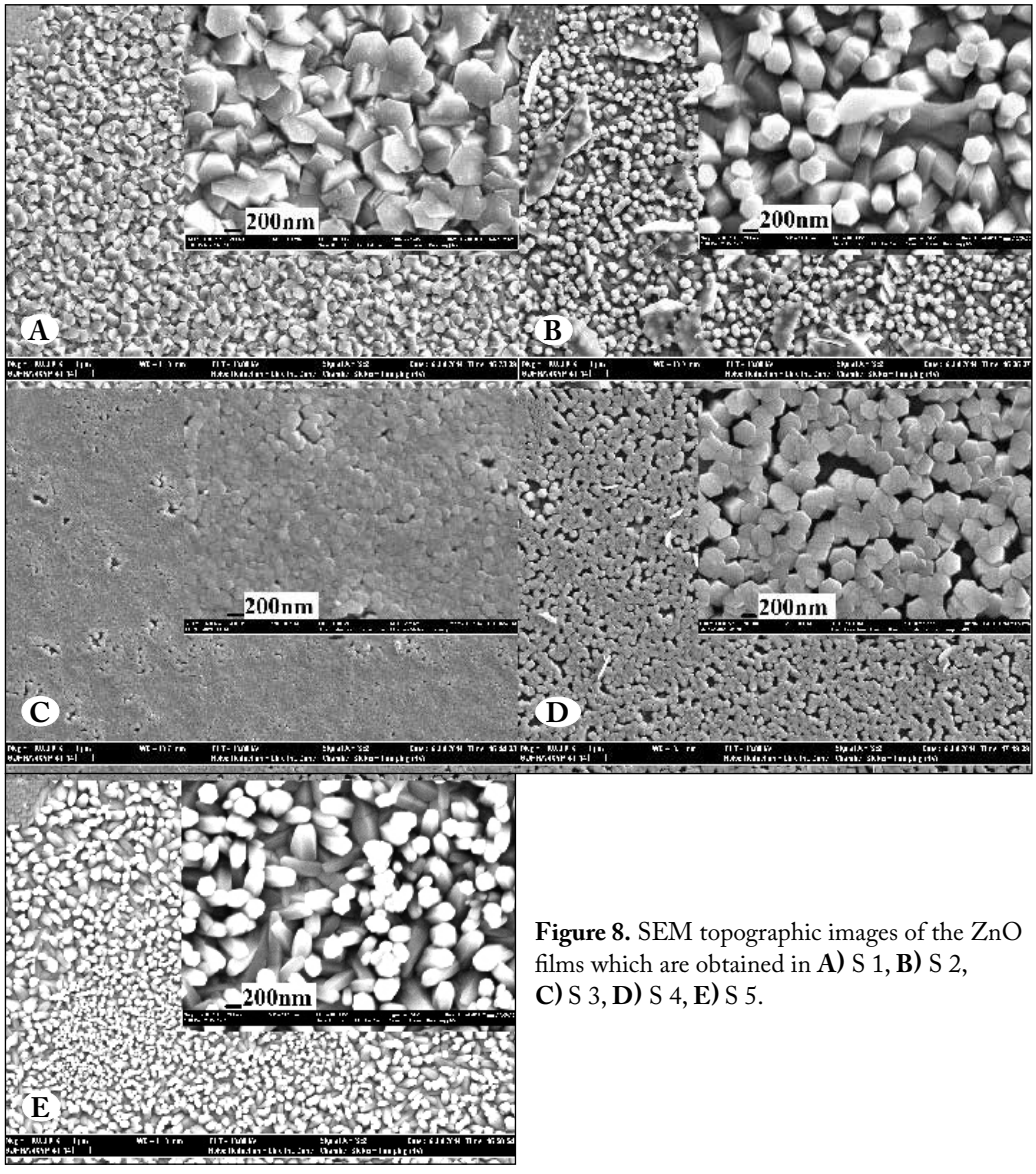

Figure 8. SEM topographic images of the ZnO films which are obtained in **A)** S 1, **B)** S 2, **C)** S 3, **D)** S 4, **E)** S 5.

It is shown from the Figure 8a that ZnO particles formed in polymorphic form with an average 600 nm size and the surface of the other films of S series were covered with nanorods. On the surface of the film obtained at -0.99 V the rods are very dense and this film is very compact but the surfaces of the films produced at below or above of -0.99 V were covered with sparse nanorods. The surface images of the films produced under magnetic field are given in Figure 9. It is shown from the Figure 9 that surfaces of the films obtained at -0.90 V, -0.99 V and -1.05 V were covered with fibrous cable like structure and they were formed in dense and compact form. On the other hand when the film was produced at -1.16 V, the surface consisted of lace like structure. In the literature, there is no both fibrous cable and lace like structure.

4. Conclusion

In this work, ZnO films were produced both without magnetic field and under magnetic field for different cathodic voltages and were compared each other. The structural analyses were studied by XRD. The XRD results showed that when the magnetic field was applied, the crystallite sizes decreased from an average of 44 nm to anaverage of 37 nm. The magnetic field may scatter ions in the solutions and therefore it may effect the crystallization of the films and naturally crystallite sizes. Magnetic field also changed the optical properties,which are measured by UV-vis spectrophotometer, such as band gap. The energy gaps of the films produced without magnetic field varied between 3.50 and 3.63 eV and the relation between the band gap and

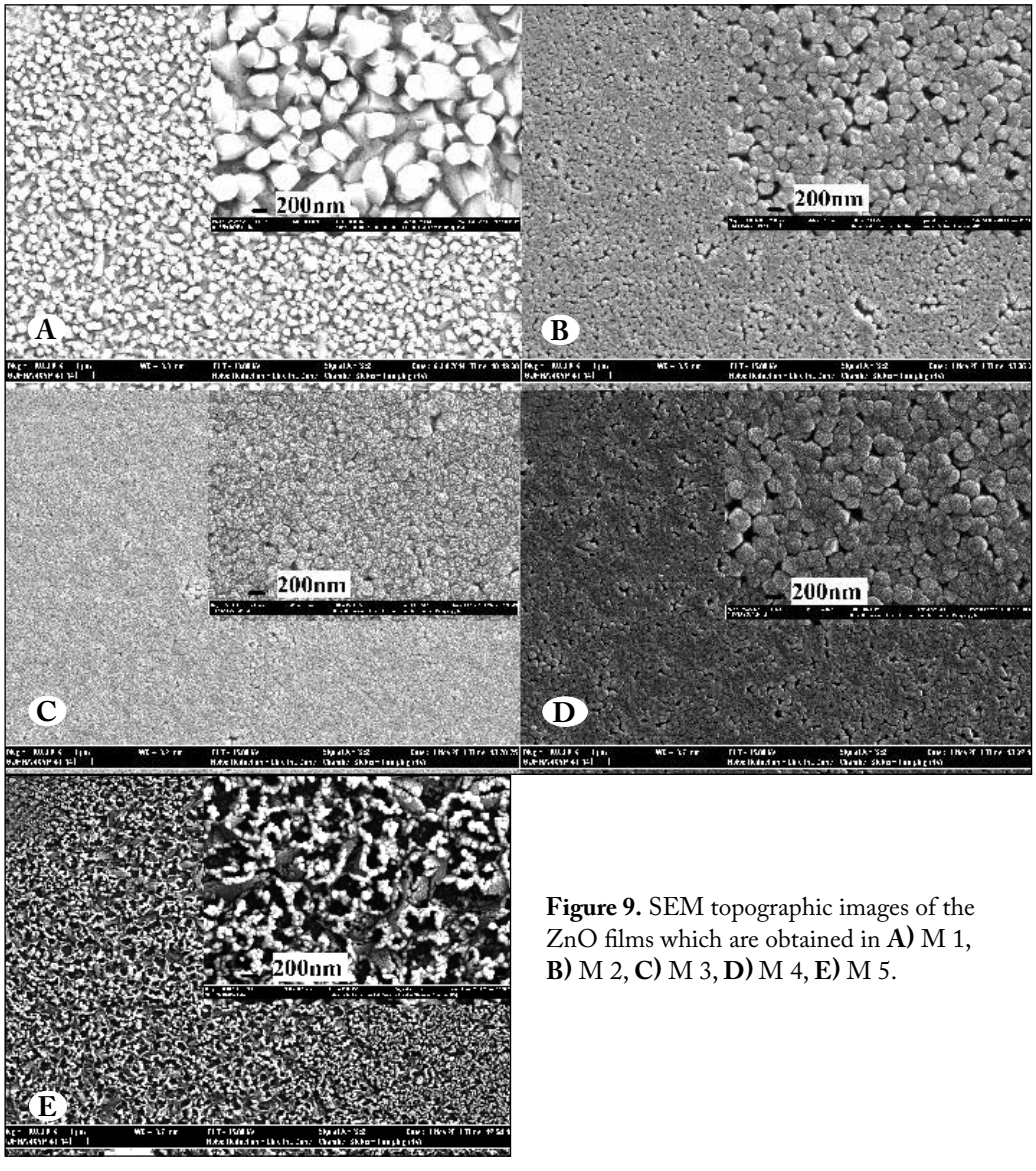

Figure 9. SEM topographic images of the ZnO films which are obtained in **A)** M 1, **B)** M 2, **C)** M 3, **D)** M 4, **E)** M 5.

cathodic voltage wasn't established. On the other hand there are relation between band gap and cathodic potential when ZnO films were produced under magnetic field. As cathodic voltage decreased from -1.16 V to -0.80 V the band gap increased from 3.60 eV to the 3.79 eV proportionally. These values are higher than the band gaps of the films produced without a magnetic field. Therefore, it may be say that the ZnO samples get suitable for gas sensors. The morphological properties were investigated using SEM images. The SEM images showed that fibrous cable like and lace like structures can be produced under magnetic field. On the other hand it may be say that surface area might be increased by applying magnetic field. Increasing surface area may be suitable for optoelectronic devices.

5. References

AlArfaj, E. Subahi, A. 2015. The influence of external magnetic field on the structural and optical properties of nanocrystalline ZnO thin films prepared by dip coating method. *Superlattice Microst.*, 86: 508-517.

Altıokka, B. Kıyak Yıldırım, A. 2016. Effects of External Alternating Magnetic Field on ZnO Films Obtained by Electrodeposition. *Arab. J. Sci. Eng.*, 41: 2345-2351.

Ezenwa, IA. 2012. Synthesis and Optical Characterization of Zinc Oxide Thin Film. *Res. J. Chem. Sci.,* 2: 26-30.

Henni, A. Merrouche, A. Telli, L. Karar, A. 2016. Studies on the structural, morphological, optical and electrical properties of Al-doped ZnO nanorods prepared by electrochemical deposition. *J. Electroanal. Chem.*, 763: 149-154.

Jan, T. Iqbal, J, Ismail, M. Zakaullah, M. Naqvi, SH. Badshah, N. 2013. Sn doping induced enhancement in the activity of ZnO nanostructures against antibiotic resistant S. aureus bacteria. *Int. J. Nanomed.*, 8: 3679-3687.

Mahdi, EM. Hamdi, M. Meor Yusoff, MS. 2013. The Effect of Sintering on the Physical and Optical Properties of Nano-TiO2 Synthesized Via a Modified Hydrothermal Route. *Arab. J. Sci. Eng.*, 38: 1701-1711.

Park, Y. Nam, G. Leem, JY. 2015. Effect of a Sn Seed Layer and ZnCl2 Concentration on Electrodeposited ZnO Nanostructures. *J. Korean Phys. Soc.*, 66: 1253-1258.

Sun, S. Jiao, S. Zhang, K. Wang, D. Gao, S. Li, H. Wang, J. Yu, Q. Guo, F. Zhao, L. 2012. Nucleation effect and growth mechanism of ZnO nanostructures by electrodeposition from aqueous zinc nitrate baths. *J. Cryst. Growth,* 359: 15-19.

Valdés, MH. Berruet, M. Goossens, A. Vázquez, M. 2010. Spray deposition of CuInS2 on electrodeposited ZnO for low-cost solar cells. *Surf. Coat. Tech.*, 204: 3995-4000

Wei, M. Li, CF. Deng, H. Deng, XR. 2012. A photoconductor based on heavily Al-doped nano-ZnO thin film and its application to a chaos generator. *J. Chin. Inst. Eng.*, 35: 1065-1069.

Wen-Bo, W. Hang, G. Xing-Li, H. Wei-Peng, X. Jin-Kai, C. Xiao-Zhi, W. Ji-Kui, L. 2015. Transparent ZnO/glass surface acoustic wave based high performance ultraviolet light sensors. *Chin. Phys.,* 24: 57701-57705

Yilmaz, M. Tatar, D. Sonmez, E. Cirak, C. Aydogan, S. Gunturkun, R. 2016. Investigation of Structural, Morphological, Optical, and Electrical Properties of Al Doped ZnO Thin Films Via Spin Coating Technique. *Syn. React.* İnorg. *Met*. http://dx.doi.org/10.1080/15533174.2014.988795

Zhang, M. Xu, K. Jiang, X. Yang, L. He, G. Song, X. Sun, Z. Lv, J. 2014. Effect of methanol ratio in mixed solvents on optical properties and wettability of ZnO films by cathodic electrodeposition. *J. Alloy Compd.*, 615: 327-332.